Scenarios for Gluino Coannihilation

John Ellis[1,2], **Jason L. Evans**[3,4], **Feng Luo**[2] and **Keith A. Olive**[3,4]

[1] *Theoretical Particle Physics and Cosmology Group, Department of Physics,*
King's College London, London WC2R 2LS, United Kingdom

[2] *Theory Division, CERN, CH-1211 Geneva 23, Switzerland*

[3] *School of Physics and Astronomy, University of Minnesota, Minneapolis, MN 55455, USA*

[4] *William I. Fine Theoretical Physics Institute, School of Physics and Astronomy,*
University of Minnesota, Minneapolis, MN 55455, USA

Abstract

We study supersymmetric scenarios in which the gluino is the next-to-lightest supersymmetric particle (NLSP), with a mass sufficiently close to that of the lightest supersymmetric particle (LSP) that gluino coannihilation becomes important. One of these scenarios is the MSSM with soft supersymmetry-breaking squark and slepton masses that are universal at an input GUT renormalization scale, but with non-universal gaugino masses. The other scenario is an extension of the MSSM to include vector-like supermultiplets. In both scenarios, we identify the regions of parameter space where gluino coannihilation is important, and discuss their relations to other regions of parameter space where other mechanisms bring the dark matter density into the range allowed by cosmology. In the case of the non-universal MSSM scenario, we find that the allowed range of parameter space is constrained by the requirement of electroweak symmetry breaking, the avoidance of a charged LSP and the measured mass of the Higgs boson, in particular, as well as the appearance of other dark matter (co)annihilation processes. Nevertheless, LSP masses $m_\chi \lesssim 8$ TeV with the correct dark matter density are quite possible. In the case of pure gravity mediation with additional vector-like supermultiplets, changes to the anomaly-mediated gluino mass and the threshold effects associated with these states can make the gluino almost degenerate with the LSP, and we find a similar upper bound.

October 2015

1   Introduction

The absence of supersymmetry so far, at LHC Run I [1, 2] and elsewhere, raises the question where, if anywhere, is it hiding. There are scenarios for which, at least, some supersymmetric particles were produced in LHC Run I, but have been overlooked. Examples include models where R-parity is violated [3], or the spectra are compressed [4, 5]. Alternatively, sparticles might be too heavy to have been detected at LHC Run I, but might be within range of future LHC runs [6]. It is also possible that supersymmetric particles may lie beyond the reach of the LHC altogether, and require a future higher-energy pp collider for its detection.

If one assumes that R-parity is conserved, the lightest supersymmetric particle (LSP) must be stable, and hence make at least a contribution to the cosmological cold dark matter density [7]. The total density of cold dark matter is very tightly constrained by measurements of the cosmic microwave background radiation [8]. It is clear, therefore, that the parameters of generic models are constrained in very specific ways in order to realize the correct dark matter density [9, 10, 11, 12]. Moreover, this parameter space with the correct density is likely to be found in a region of parameter space where the density varies rapidly with the parameters. In these cases, regions where the LSP contributes only a fraction of the cold dark matter density will have parameters similar to those regions yielding the correct total density.

This sensitivity of the dark matter density to parameters are particularly relevant for models with compressed and/or very heavy spectra that have survived LHC searches. Examples of specific choices of heavy spectra that yield the correct cosmological dark matter density include scenarios in which the LSP, χ, would have annihilated with itself through a direct-channel boson such as the heavier neutral Higgs bosons A and H [13]. Alternatively, there might be one or more heavier supersymmetric particles that are nearly degenerate with the LSP, χ, and would have coannihilated with it in the early Universe [14]. There are several examples of possible coannihilating sparticles, including the lighter stau, or possibly some other slepton [15], the lighter stop squark [16, 17, 18], the lighter chargino [19, 17] and the gluino [20, 21, 22, 23, 24, 25, 18, 26].

In most cases, coannihilation with a sparticle having stronger interactions extends the allowed mass range of the LSP. The possibility of gluino coannihilation is therefore particularly interesting since it interacts strongly suggesting it can accommodate a heavier LSP than is possible from coannihilation with a stau or slepton. In fact, it has been shown that a dark matter density realized by an LSP coannihilating with the gluino could lie well beyond the reach of the LHC, with a mass as heavy as $m_\chi \lesssim 8$ TeV [26].

The possibility of gluino coannihilation does not arise in the minimal supersymmetric extension of the Standard Model (MSSM) with the soft supersymmetry-breaking parameters constrained to be universal at the input GUT scale (the CMSSM) [13, 27, 28, 29, 9, 30], nor in related models with non-universal Higgs masses [31, 28, 32, 33, 34]. However, as we discuss in this paper, gluino coannihilation can become important in variants of the MSSM with non-universal gaugino masses, and in variations of pure gravity mediation (PGM) with non-minimal matter content such as additional vector-like supermultiplets [22, 23].

The layout of this paper is as follows. In Section 2 we set out the coupled set of Boltzmann equations that we use to calculate the relic LSP density, discussing the circumstances under which the analysis can be reduced to a single Boltzmann equation for a particular combination of sparticle abundances [26]. Then, in Section 3 we discuss various scenarios with non-universal gaugino masses in which gluino coannihilation can become important, delineating the corresponding strips in parameter space and comparing their extents with the results of [26]. We find that this scenario is constrained by the requirement of consistent electroweak symmetry breaking (EWSB), by the measurement of m_H, and by avoidance of a stop or chargino LSP. We give examples showing that the correct dark matter density is possible with LSP masses as large as 8 TeV. Section 4 contains a similar analysis of PGM models with vector-like supermultiplets, focusing on an example with a single extra pair of **10** and **$\overline{10}$** representations of SU(5). Because the anomaly-mediated contribution to the gluino mass is zero in this case, threshold effects due to these additional states generate almost the entire gluino mass. This suppresses the gluino mass relative to those of the other gauginos, leading to near-degeneracy between the gluino and the LSP. Neutralino dark matter candidates with similarly large values of m_χ are again possible. Finally, Section 5 summarizes our conclusions and discusses the prospects for discovering supersymmetry in these gluino coannihilation scenarios.

2 Calculations of Gluino Coannihilation

In this section, we present general formulae for calculating the dark matter thermal relic density, and then specialize it to the case of the gluino coannihilation scenarios we consider in this paper, taking into account the effects of gluino-gluino bound states.

We consider N R-odd species in the thermal bath in the early Universe. We assume that the rates for interconverting the LSP (which is labeled as the first species, with mass m_1) and the first l species ($1 \leq l \leq N$) are sufficiently large, compared to the Hubble expansion rate, that to a very good approximation the ratios of densities are equal to the equilibrium

ratios: $n_i/n_1 = n_i^{eq}/n_1^{eq}$ for $(i = 1, ..., l)$.

For any of the N species, the evolution of its number density is governed by the Boltzmann equation

$$\frac{dn_i}{dt} + 3H(T)n_i = -\sum_{j=1}^{N} \langle \sigma v \rangle_{ij \to SM} \left(n_i n_j - n_i^{eq} n_j^{eq}\right) - \sum_{\substack{j=1 \\ j \neq i}}^{N} \langle \Gamma \rangle_{i \to j} \left(n_i - n_i^{eq} \frac{n_j}{n_j^{eq}}\right), \tag{1}$$

where $\langle \sigma v \rangle_{ij \to SM}$ is the product of the thermally-averaged relative velocity with the total cross section for the channels of i and j (co)annihilating into Standard Model particles, and $\langle \Gamma \rangle_{i \to j}$ is the sum of all the thermally-averaged decay and conversion rates for decay and conversion processes for which there is one particle i in the initial state and one particle j in the final state, with all other particles involved in these processes being Standard Model particles. The relations between the thermally-averaged forward and backward reactions are used in (1), and we assume for all the Standard Model particles involved that $n_{SM} = n_{SM}^{eq}$, so that, for example,

$$\langle \Gamma \rangle_{i \to j} n_i^{eq} = \langle \Gamma \rangle_{j \to i} n_j^{eq}. \tag{2}$$

Written in terms of the yields, $Y_i \equiv n_i/s$, (1) becomes

$$\frac{dY_i}{dx} = -\frac{xs}{H(m_1)} \left(1 + \frac{T}{3g_{*s}} \frac{dg_{*s}}{dT}\right) \left[\sum_{j=1}^{N} \langle \sigma v \rangle_{ij \to SM} \left(Y_i Y_j - Y_i^{eq} Y_j^{eq}\right) + \sum_{\substack{j=1 \\ j \neq i}}^{N} \frac{\langle \Gamma \rangle_{i \to j}}{s} \left(Y_i - Y_i^{eq} \frac{Y_j}{Y_j^{eq}}\right)\right], \tag{3}$$

where

$$x \equiv \frac{m_1}{T}, \; s = \frac{2\pi^2}{45} g_{*s} T^3, \; H(m_1) \equiv H(T)x^2 = \left(\frac{4\pi^3 G_N g_*}{45}\right)^{\frac{1}{2}} m_1^2, \tag{4}$$

and g_{*s} and g_* are the total numbers of effectively massless degrees of freedom associated with the entropy density and the energy density, respectively.

Defining $\tilde{Y} \equiv \sum_{i=1}^{l} Y_i$, $\Delta_i \equiv (m_i - m_1)/m_1$ and $\tilde{g}_{eff} \equiv \sum_{i=1}^{l} g_i (1 + \Delta_i)^{3/2} e^{-\Delta_i x}$, we have

$$\frac{Y_i^{eq}}{\tilde{Y}^{eq}} = \frac{g_i \left(\frac{m_i T}{2\pi}\right)^{3/2} e^{-m_i/T}}{\sum_{j=1}^{l} g_j \left(\frac{m_j T}{2\pi}\right)^{3/2} e^{-m_j/T}} = \frac{g_i (1 + \Delta_i)^{3/2} e^{-\Delta_i x}}{\tilde{g}_{eff}}. \tag{5}$$

Using $Y_i/\tilde{Y} = Y_i^{eq}/\tilde{Y}^{eq}$ for $i = 1, ..., l$ and summing over (3) for the first l species, we find

$$\begin{aligned}
\frac{d\tilde{Y}}{dx} &= -\frac{xs}{H(m_1)} \left(1 + \frac{T}{3g_{*s}} \frac{dg_{*s}}{dT}\right) \left\{\langle \tilde{\sigma}_{eff} v \rangle \left(\tilde{Y}^2 - \tilde{Y}_{eq}^2\right)\right. \\
&\quad \left. + \sum_{k=l+1}^{N} \left[\langle \sigma_{keff} v \rangle \left(\tilde{Y} Y_k - \tilde{Y}^{eq} Y_k^{eq}\right) + \frac{\langle \Gamma_k \rangle_{eff}}{s} \left(\tilde{Y} - \tilde{Y}^{eq} \frac{Y_k}{Y_k^{eq}}\right)\right]\right\},
\end{aligned} \tag{6}$$

while for each of the species k $(l < k \leq N)$, we get

$$
\begin{aligned}
\frac{dY_k}{dx} = & -\frac{xs}{H(m_1)} \left(1 + \frac{T}{3g_{*s}} \frac{dg_{*s}}{dT}\right) \left\{ \langle \sigma_{keff} v \rangle \left(\tilde{Y} Y_k - \tilde{Y}^{eq} Y_k^{eq} \right) \right. \\
& + \sum_{j=l+1}^{N} \langle \sigma v \rangle_{kj \to SM} \left(Y_k Y_j - Y_k^{eq} Y_j^{eq} \right) - \frac{\langle \Gamma_k \rangle_{eff}}{s} \left(\tilde{Y} - \tilde{Y}^{eq} \frac{Y_k}{Y_k^{eq}} \right) \\
& + \left. \sum_{\substack{j=l+1 \\ j \neq k}}^{N} \frac{\langle \Gamma \rangle_{k \to j}}{s} \left(Y_k - Y_k^{eq} \frac{Y_j}{Y_j^{eq}} \right) \right\},
\end{aligned}
\tag{7}
$$

where

$$
\langle \sigma_{keff} v \rangle \equiv \sum_{i=1}^{l} \langle \sigma v \rangle_{ik \to SM} \frac{Y_i^{eq}}{\tilde{Y}^{eq}} = \sum_{i=1}^{l} \langle \sigma v \rangle_{ik \to SM} \frac{g_i (1 + \Delta_i)^{3/2} e^{-\Delta_i x}}{\tilde{g}_{eff}}, \tag{8}
$$

$$
\langle \Gamma_k \rangle_{eff} \equiv \sum_{i=1}^{l} \langle \Gamma \rangle_{i \to k} \frac{Y_i^{eq}}{\tilde{Y}^{eq}} = \sum_{i=1}^{l} \langle \Gamma \rangle_{i \to k} \frac{g_i (1 + \Delta_i)^{3/2} e^{-\Delta_i x}}{\tilde{g}_{eff}}, \tag{9}
$$

$$
\langle \tilde{\sigma}_{eff} v \rangle \equiv \sum_{i,j=1}^{l} \langle \sigma v \rangle_{ij \to SM} \frac{Y_i^{eq} Y_j^{eq}}{\tilde{Y}_{eq}^2} = \sum_{i,j=1}^{l} \langle \sigma v \rangle_{ij \to SM} \frac{g_i g_j (1 + \Delta_i)^{3/2} (1 + \Delta_j)^{3/2} e^{-(\Delta_i + \Delta_j)x}}{\tilde{g}_{eff}^2}. \tag{10}
$$

We note that in the case $N = l+1$, the final term in (7) does not appear. In the case $N = l$, (6) does not have the two terms in the squared bracket, and reverts to the familiar form for coannihilations when all the N species are sufficiently coupled to the LSP.

We now specialize the above general formulae to the gluino coannihilation scenarios we consider in this paper. First of all, following the discussion in [26], the effect of gluino-gluino bound states on the calculation of the dark matter relic density can be taken into account simply by modifying the Boltzmann equation by including the Sommerfeld-enhanced thermal-averaged velocity-weighted gluino pair annihilation cross section [24], which includes gluino-pair annihilation to two gluons and to all the quark anti-quark pair channels:

$$
\langle \sigma v \rangle_{\tilde{g}\tilde{g} \to gg, q\bar{q}} \to \langle \sigma v \rangle_{\tilde{g}\tilde{g} \, incl. \, \tilde{R}} \equiv \langle \sigma v \rangle_{\tilde{g}\tilde{g} \to gg, q\bar{q}} + \langle \sigma v \rangle_{bsf} \frac{\langle \Gamma \rangle_{\tilde{R}}}{\langle \Gamma \rangle_{\tilde{R}} + \langle \Gamma \rangle_{dis}}, \tag{11}
$$

where $\langle \sigma v \rangle_{bsf}$, $\langle \Gamma \rangle_{\tilde{R}}$ and $\langle \Gamma \rangle_{dis}$ are the thermally-averaged formation cross section, decay rate and dissociation rate for the bound state $\tilde{R}$, respectively. The details of these quantities and the derivation of eq. (11) can be found in Section 3, 5 and Appendix B of [26].

When the rate for interconverting the neutralino LSP and the gluino is sufficiently large, compared to the Hubble rate, so that to a good approximation the relation $Y_{\tilde{g}}(T)/Y_1(T) =$

$Y_{\tilde{g}}^{eq}(T)/Y_1^{eq}(T)$ holds at all temperatures during which the sum of $Y_{\tilde{g}}(T)$ and $Y_1(T)$ changes non-negligibly, we can use a single Boltzmann equation to solve for the dark matter relic abundance, including the gluino species in $\tilde{Y}$ and $\langle\tilde{\sigma}_{eff}v\rangle$ and using (6) without the two terms in the squared bracket. Otherwise, one should use a coupled set of Boltzmann equations, namely (6) and (7), to solve for the dark matter relic abundance. For the scenarios considered in this paper, any of the R-odd species apart from the gluino is either sufficiently coupled to the LSP by having a Standard Model particle in the propagator of a tree-level Feynman diagram describing its interconversion with the LSP, or is so heavy compared to the LSP that it is effectively not participating coannihilations. Therefore, when using a coupled set of Boltzmann equations, we have $N = l + 1$ in (6) and (7), and the index k is for the gluino.

We end this Section by emphasizing that, in principle, the coupled set of Boltzmann equations can always be used to solve for the dark matter relic density, whether the rate for interconverting the gluino and the LSP is sufficiently large compared to the Hubble rate or not. However, for the former case, solving a single Boltzmann equation is usually easier than solving the coupled ones and requires less computing time.

3   The Non-Universal MSSM Scenario

It was assumed in [26] that the squarks were all degenerate with a common mass $m_{\tilde{q}}$, and the effects of sparticles with only electroweak interactions were neglected. It was found in [26] that in the presence of gluino coannihilation, a Bino LSP, χ, could be the dark matter of the universe if it weighed $\lesssim 8$ TeV, the exact value depending on the ratio $m_{\tilde{q}}/m_\chi$, with smaller values of m_χ being found for $m_{\tilde{q}}/m_\chi \lesssim 5$ and $\gtrsim 100$. Here we make a more complete study in a variant of the MSSM with universal soft supersymmetry-breaking scalar masses m_0 and trilinear couplings A_0, allowing a restricted form of non-universality in the gaugino sector with $M_1 = M_2 \neq M_3$ at the input GUT scale. The results therefore depend on M_1/M_3 as well as the usual CMSSM parameters m_0, A_0 and $\tan\beta$ (the ratio of MSSM Higgs vev's). This is therefore a one-parameter extension of the CMSSM (with the new free parameter being M_3) as is the NUHM1 (with the soft Higgs masses $m_1 = m_2 \neq m_0$) [33, 34]. We consider in this section various (M_1, M_3) planes for various choices of the other parameters which illustrate the range of possibilities.

We first consider the example with $m_0 = 1000$ TeV, $A_0/m_0 = 1.5$ and $\tan\beta = 2.5$ shown in Fig. 1. In the left panel and in subsequent figures, the regions where the relic LSP density $\Omega_\chi h^2$ falls within the range allowed by Planck and other data are shown as dark blue strips, and the regions where the lightest neutralino is no longer the LSP are shaded brick-red. In
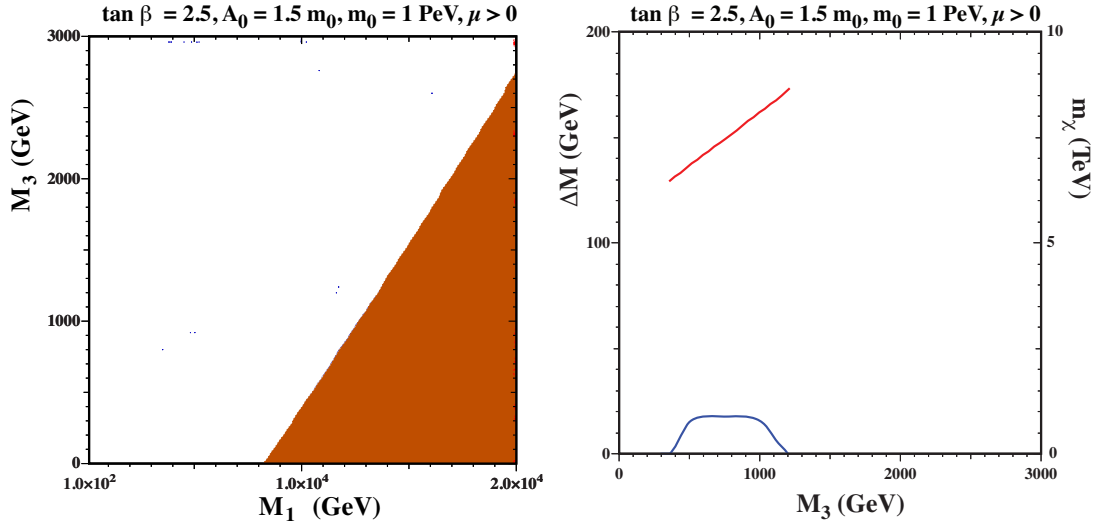
Figure 1: *The (M_1, M_3) plane (left) for $m_0 = 1000$ TeV, $A_0/m_0 = 1.5$ and $\tan\beta = 2.5$. The dark blue strip in the left panel shows where the relic LSP density $\Omega_\chi h^2$ falls within the ± 3-σ range allowed by Planck and other data, and the lightest neutralino is no longer the LSP in the regions shaded brick-red. The right panel shows the gluino-neutralino mass difference (left axis, blue line) and the neutralino mass (right axis, red line) as functions of M_3.*

this case, the gluino is the LSP in the shaded region. Because of the scale of the plot, it is difficult to discern the relic density strip, which lies very close to the boundary of this region. However, we note that it lies to the left of the red shaded region only when M_3 is between ~ 400 and ~ 1200 GeV, as shown in the right panel of Fig. 1 by the left axis and blue curve, which shows the mass difference $\Delta M \equiv m_{\tilde{g}} - m_\chi$ between the gluino and the neutralino along the coannihilation strip as a function of the input gluino mass. Also shown in the right panel (as a red line) is the neutralino mass as a function of M_3. As seen in Fig. 6 in [26], the choice of m_0 in Fig. 1 corresponds to values of $m_{\tilde{g}}/m_\chi$ extending from beyond the plateau at small M_3 to values along the plateau at large M_3. The gluino coannihilation strip therefore has two end-points where $\Delta M \to 0$, corresponding to the limiting values $m_\chi \sim 6$ TeV and $m_\chi \sim 8$ TeV seen in the right panel of Fig. 1: for larger and smaller M_3, $\Delta M < 0$ and the gluino is the LSP.

We note that the Higgs mass is relatively insensitive to the choice of M_1 and M_3, and therefore varies very little across the plane with $\tan\beta$, A_0, and m_0 fixed [1]. For the case shown in Fig. 1, we calculate $m_H \approx 126.3$ GeV, which is compatible with the experimental measurement, within the theoretical uncertainties. We do not show any other (M_1, M_3) planes for

---

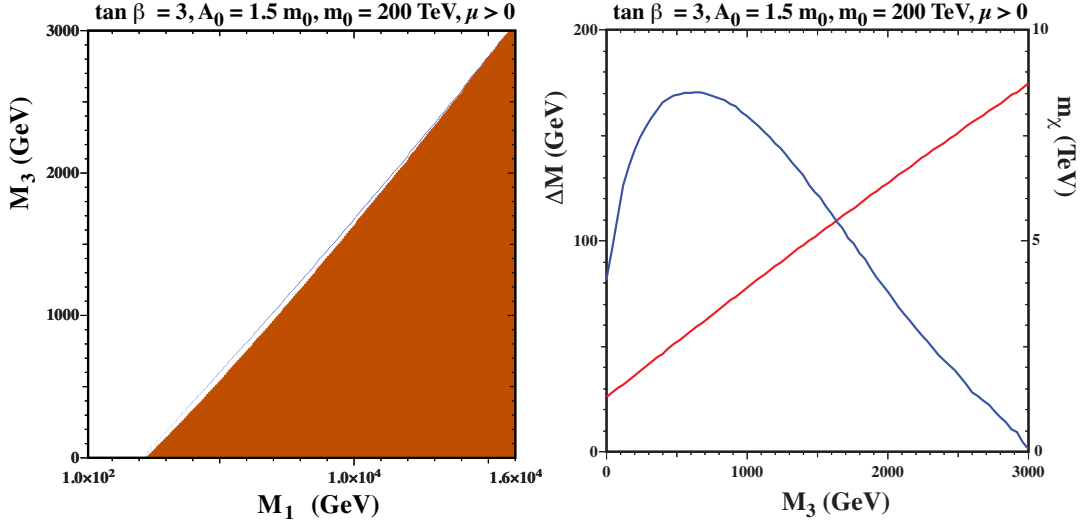[1]We calculate the Higgs mass using the procedure outlined in [35].

Figure 2: *As for Fig. 1, but for $m_0 = 200$ TeV and $A_0/m_0 = 1.5$, with $\tan\beta = 3$.*

$m_0 = 1000$ TeV, since the possibilities are quite limited: there are no consistent solutions of the electroweak symmetry-breaking conditions for much smaller values of $A_0/m_0 \lesssim 1$ and/or larger values of $\tan\beta$, and m_H is too large for larger values of $\tan\beta$ and/or A_0/m_0 (though it increases quite slowly with A_0).

We consider next an example of a (M_1, M_3) plane for $m_0 = 200$ TeV, which corresponds to values of $m_{\tilde{q}}/m_\chi$ along the plateau in [26]. The left panel of Fig. 2 shows the (M_1, M_3) plane for $\tan\beta = 3$ and $A_0/m_0 = 1.5$. In this case there is a longer gluino coannihilation strip extending nearly all the way to $M_3 \sim 3$ TeV. The panel on the right again shows the gluino-neutralino mass difference ΔM (blue line) which in this case peaks at approximately 170 GeV, which is consistent with the results of [26] for intermediate squark-to-gluino mass ratios. Also shown is the neutralino mass as a function of M_3 (red line): it again rises to $m_\chi \sim 8$ TeV at the tip of the coannihilation strip, which has M_3 slightly > 3 TeV.

The Higgs mass in this case is again very slowly varying across the plane and takes the value $m_H \sim 125$ GeV for this choice of $\tan\beta = 3$. In comparison, had we chosen $\tan\beta = 5$, the (M_1, M_3) plane would look almost identical but with $m_H \sim 131$ GeV. This and larger values of $\tan\beta$ are therefore excluded for this value of A_0/m_0. We have also studied smaller values of A_0/m_0 and found no consistent solutions of the electroweak symmetry-breaking conditions for $M_3 \lesssim 500$ GeV for $A_0/m_0 = 1$ and no consistent solutions across the plane at somewhat lower A_0/m_0. This is also the case for $\tan\beta = 10$ and $A_0/m_0 = 1.5$, for which $m_H \sim 134$ GeV. Larger values of A_0/m_0 also give values that tend to increase m_H and, if

7

increased too much, the stop becomes the LSP and eventually tachyonic.

Next we consider some sample (M_1, M_3) planes with $m_0 = 20$ TeV and $\tan\beta = 5$, corresponding to the lower end of the m_χ plateau found in [26]. Fig. 3 is for the case $A_0/m_0 = 1$, where we see in the left panel that electroweak symmetry breaking is possible up to values of $M_1 \lesssim 14$ TeV. There is a gluino coannihilation strip close to the colored LSP boundary for $M_1 \lesssim 9$ TeV. This is terminated by a spur extending to large M_3 when 9 TeV $\lesssim M_1 \lesssim 10$ TeV, where the lighter chargino is the LSP. There is no chargino coannihilation strip along the boundary of this region at large M_3, because the relic density is too high: for these values of M_1 and M_3, the Higgsino mass is too large and other coannihilations are not sufficient to bring the relic density down. At larger values, 10 TeV $\lesssim M_1 \lesssim 11$ TeV, there is a Higgsino-gluino coannihilation strip, which is followed at larger M_1 by a focus-point strip [36] hugging the electroweak symmetry breaking boundary where the neutralino is well-tempered [37]. In this case we see both the 124 and 125 GeV Higgs mass contours and, as in the previous example, m_H is compatible with experiment whenever the dark matter density falls within the allowed range.

Because the relic density strip is a multi-valued function of M_3, the structure of the gluino-neutralino mass difference ΔM (blue curve) and the neutralino mass (red curve) shown in the right panel of Fig. 3 are more complicated than in the previous cases. After growing to a local maximum ~ 170 GeV when $M_3 \sim 1$ TeV, ΔM starts to fall at larger M_3. We then see a change in behaviour at $M_3 \approx 1800$ GeV along the gluino coannihilation strip. Here, the neutralino becomes Higgsino-like and, as M_1 is increased, the coannihilation strip tends toward lower M_3 with an increasing mass difference, as seen in the lower branch of the blue curve. A Higgsino LSP emerges for larger M_1 because it gives a positive contribution to the up Higgs soft mass from renormalization group running. As the up Higgs soft mass goes to zero so does μ and the Higgsino becomes the LSP. Once μ is small enough, the Higgsino can be a thermal relic without any assistance in setting the relic density from other particles. In this focus-point-like region, the mass difference increases beyond the range displayed. This behaviour is correlated with the value of m_χ (red curve), which increases monotonically to ~ 4 TeV. When the bino/Higgsino transition occurs at $M_3 \approx 1800$ GeV, m_χ doubles back down to $M_3 \approx 500$ GeV. Then, on the focus-point branch of the relic density strip, the LSP is mostly Higgsino, the value of M_3 grows, and the lightest neutralino mass takes the characteristic value $m_\chi \sim 1$ TeV.

In Fig. 4 we choose a larger value of $A_0/m_0 = 1.5$, and we see in the left panel a gluino coannihilation strip that extends to $M_1 \sim 14$ TeV, along which m_H varies between 124 and 126 GeV as seen by the three Higgs mass contours. The focus-point Higgsino dark matter
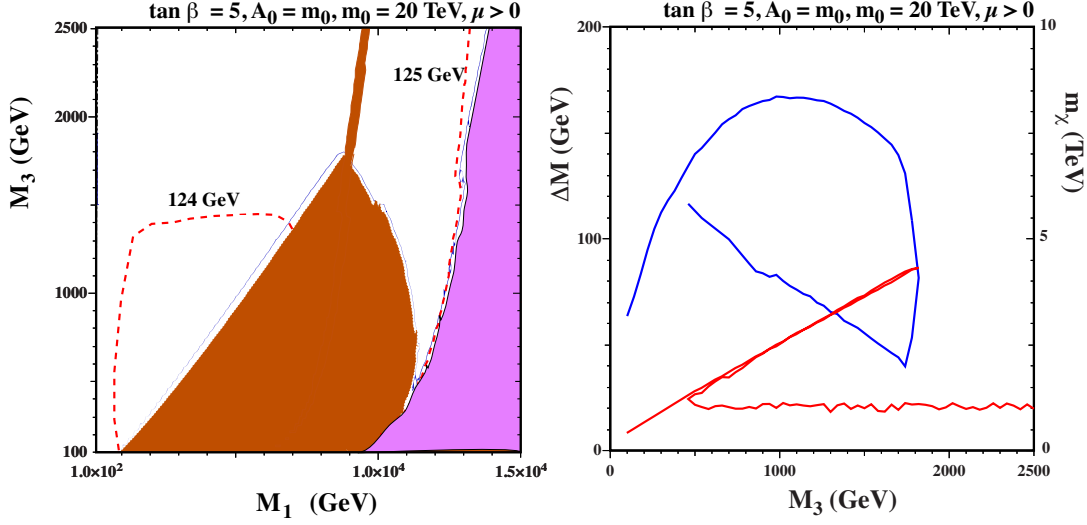
Figure 3: *As for Fig. 1, but for $m_0 = 20$ TeV and $\tan\beta = 5$ with $A_0/m_0 = 1.0$.*

region has disappeared, due to the large A_0 driving the Higgs mass to large negative values. The end-point of the gluino coannihilation strip is clearly seen in the right panel of Fig. 4, where $\Delta M \to 0$ (blue curve) at $M_3 \simeq 3300$ GeV. Qualitatively, this case is similar to that shown in Fig. 2, rather than to Fig. 3 with its truncated gluino coannihilation strip. In this case, the LSP mass (red curve) rises monotonically to $m_\chi \sim 7.5$ TeV at the end-point of the strip.
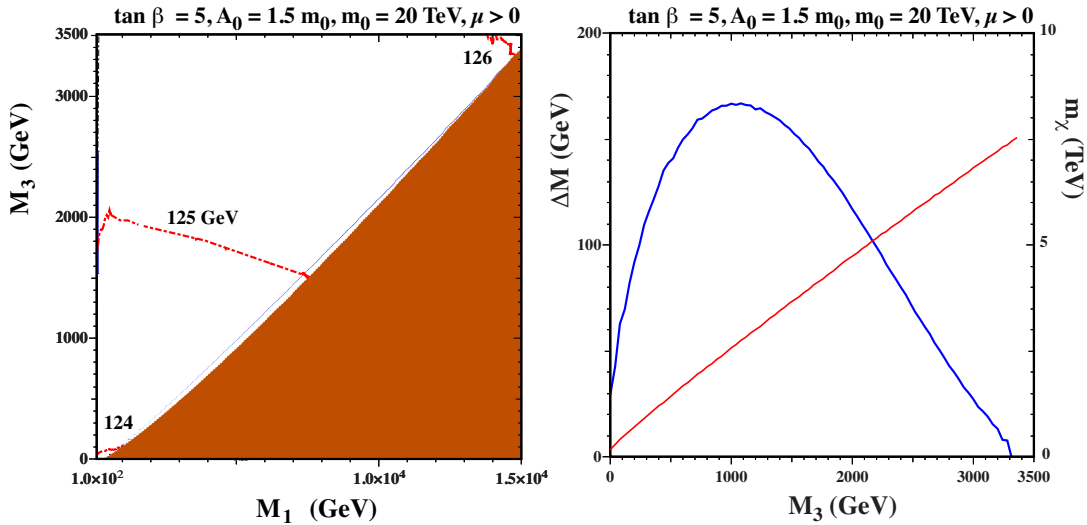

Figure 4: *As for Fig. 1, but for $m_0 = 20$ TeV and $\tan\beta = 5$ with $A_0/m_0 = 1.5$.*

9

In the left panel of Fig. 5 we display the (M_1, M_3) plane for $m_0 = 20$ TeV and $A_0/m_0 = 2$. We see again a gluino coannihilation strip, but extending only to $M_1 \sim 7.5$ TeV. It is terminated by a stop LSP region that extends to larger values of M_3 than those displayed. In principle, one might have expected to see a stop coannihilation strip running up along the boundary of the stop LSP region. However, in this case the relic density is too high along the boundary shown in this figure: as in the chargino case mentioned earlier, the would-be end-point of the stop coannihilation strip lies within the gluino LSP region. The value of m_H is generally higher than in the previous case, though compatible with experiment along all the dark matter strip. In the right panel of Fig. 5, the curves for ΔM and m_χ terminate when the stop becomes the LSP, with $m_\chi \lesssim 3.5$ TeV.
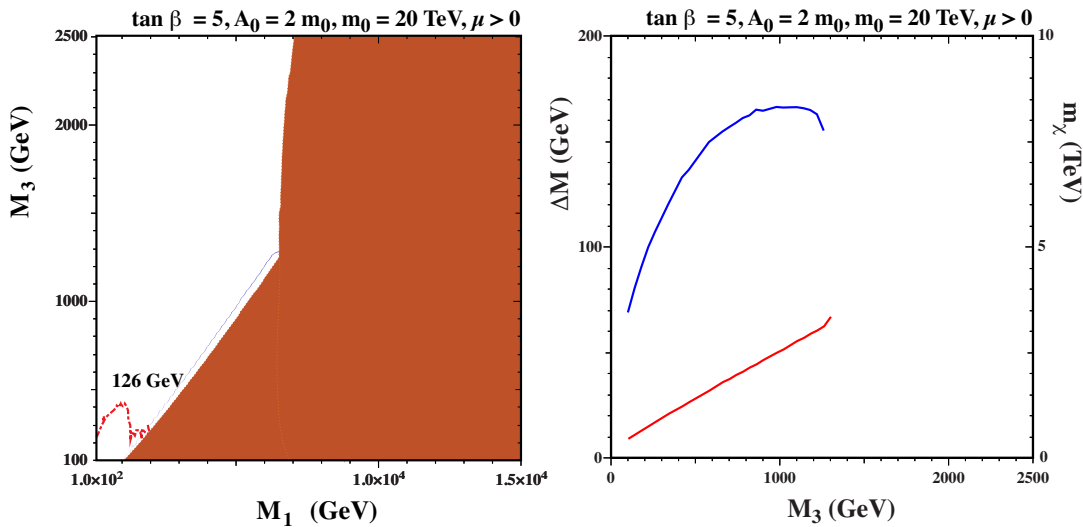

Figure 5: *As for Fig. 1, but for $m_0 = 20$ TeV and $\tan\beta = 5$ with $A_0/m_0 = 2.0$.*

In Fig. 6, we choose a lower value of $A_0/m_0 = 0.75$ and keep $\tan\beta = 5$. We see, in the left panel, that consistent electroweak symmetry breaking is possible only for relatively large M_3 and small M_1, and that there is a strip hugging the curved electroweak symmetry-breaking boundary where the LSP has an enhanced Higgsino component. Its relic density is brought into the allowed range by the same mechanism as we discussed in the case of a well-tempered neutralino. As one can see in the right panel of Fig. 6, once M_3 is large enough for EWSB solutions to exist, the mass of the lightest neutralino (which is mainly a Higgsino) is $m_\chi \sim 1.1$ TeV (red line), almost independent of M_3 for values $\gtrsim 1.1$ TeV. The gluino-neutralino mass difference does not play a role in the relic density determination and is not shown here. The red dot-dashed contour shows where $m_H = 125$ GeV: m_H is smaller

10

(larger) above (below) this contour. The Higgs mass is highly compatible with the LHC measurement all along the displayed part of the relic density strip.
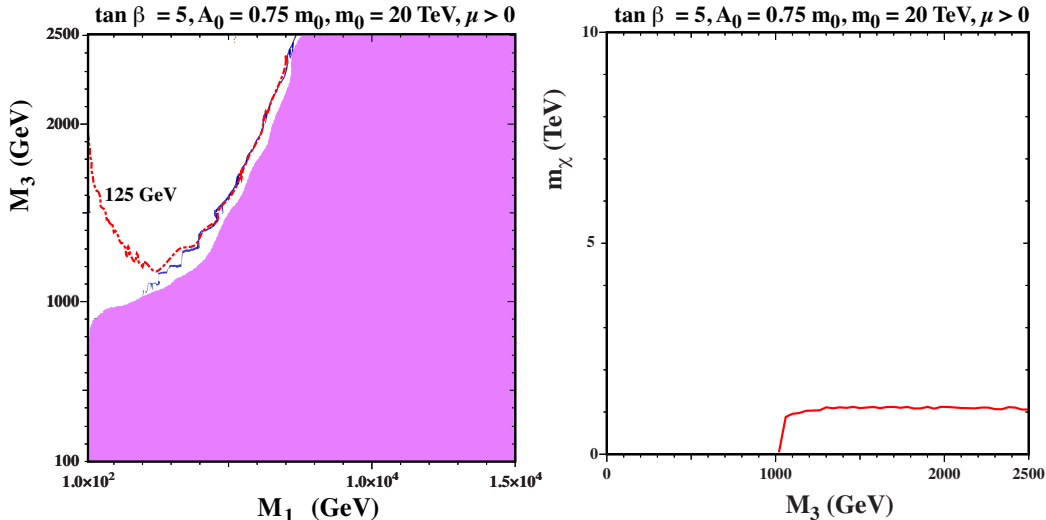

Figure 6: *As for Fig. 1, but for* $m_0 = 20$ *TeV and* $\tan\beta = 5$ *with* $A_0/m_0 = 0.75$.

At larger values of $\tan\beta$, the planes would look similar, though m_H would be larger. The (M_1, M_3) plane for $m_0 = 20$ TeV with $\tan\beta = 10$ and $A_0/m_0 = 1$ resembles that in the left panel of Fig. 6 for $\tan\beta = 5$ and $A_0/m_0 = 0.75$, with a focus-point strip following closely the curved electroweak symmetry breaking boundary. The most notable difference is the Higgs mass m_H, which is around 128 GeV and only marginally compatible with experiment after allowing for the theoretical uncertainties. For the same values of m_0 and $\tan\beta = 10$, we find no consistent electroweak symmetry breaking for smaller values of A_0/m_0, and for larger values we find that m_H is too high. Thus we find no interesting examples of gluino coannihilation for $m_0 = 20$ TeV and $\tan\beta = 10$.

Finally, we consider in Figs. 7 and 8 two examples for $m_0 = 10$ TeV, corresponding to values of $m_{\tilde{q}}/m_\chi$ below the m_χ plateau in [26]. Fig. 7 is for $\tan\beta = 10$ and $A_0/m_0 = 1$ and displays a truncated gluino coannihilation strip extending to $M_1 \sim 4$ TeV, followed by a Higgsino coannihilation strip extending to $M_1 \sim 5$ TeV, and then a focus-point strip extending beyond the limits of the plot. We find that m_H is always compatible with the experimental measurement. This example resembles that of Fig. 3 for $m_0 = 20$ TeV and $A_0/m_0 = 1$, the main difference being that the chargino spur has disappeared: we see instead a chargino LSP island at $M_1 \sim 6$ TeV and $M_3 \gtrsim 2$ TeV. As in Fig. 3, we see in the right panel that the gluino-neutralino mass difference (blue curve) has a multivalued form, and

11

becomes larger as the neutralino becomes more Higgsino-like along the gluino coannihilation strip. At larger M_1, M_3 drops along the Higgsino-gluino coannihilation strip and the mass difference increases slightly as M_3 decreases, increasing beyond the displayed range as one moves on to the focus point strip. Similarly, the neutralino mass rises as M_1 is increased, then falls back to about 1.1 TeV when the LSP is mostly a Higgsino.
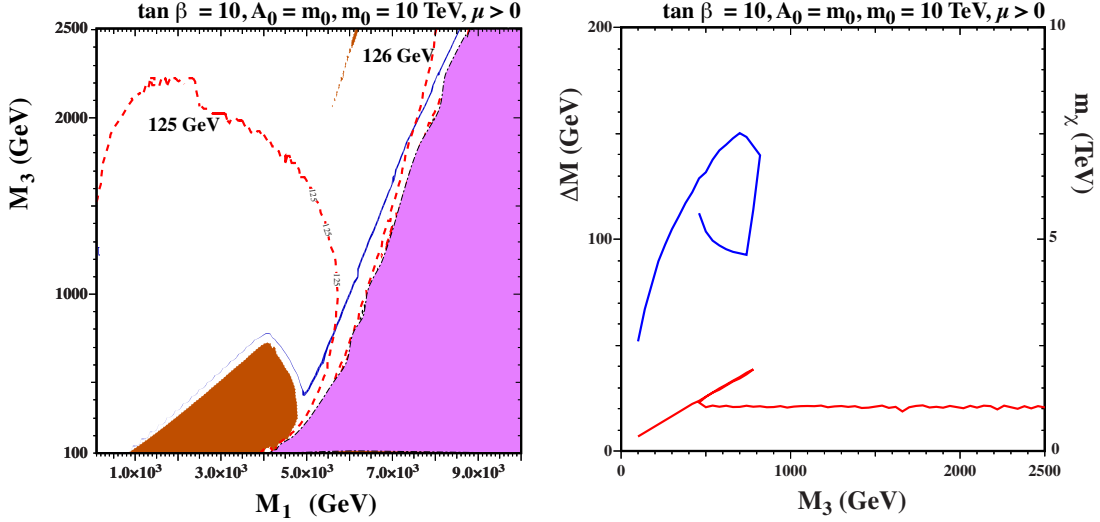

Figure 7: *As for Fig. 1, but for $m_0 = 10$ TeV, $\tan\beta = 10$ and $A_0/m_0 = 1.0$.*

Fig. 8 for $A_0/m_0 = 1.5$ displays a more extended gluino coannihilation strip reaching $M_1 \sim 7$ TeV and $m_\chi \sim 3.5$ TeV, where it is terminated by a stop LSP region. This stop LSP region would dominate for larger values of A_0/m_0, and the range of m_H would also become too high. At lower $\tan\beta$, the figures would look similar, but with a smaller Higgs mass. For example, for $\tan\beta = 5$, with $A_0/m_0 = 1.5$ (as in Fig. 8), the Higgs mass would drop by roughly 3 GeV. Lower values of $\tan\beta$ would have m_H too small, and lower values of A_0/m_0 but the same value of $\tan\beta$ would have no electroweak symmetry breaking solutions, while the stop LSP region would dominate for larger A_0/m_0.

Our analysis of gluino coannihilation in non-universal MSSM scenarios with $M_1 \neq M_3$ has shown that large values of $m_\chi \lesssim 8$ TeV are certainly possible, though restricted by competing mechanisms. This possibility occurs when $m_0 = 1000$ TeV, but only for $A_0/m_0 \sim 1.5$ and low values of $\tan\beta \lesssim 3$. The possibility of gluino coannihilation becomes more prominent for $m_0 = 200$ TeV, appearing for an extended range of $\tan\beta$ though still only for $A_0/m_0 \sim 1.5$. Gluino coannihilation is also prominent for $m_0 = 20$ TeV and $\tan\beta = 5$, but the focus point may also be important (it becomes dominant when $\tan\beta = 10$), as is Higgsino coannihilation.
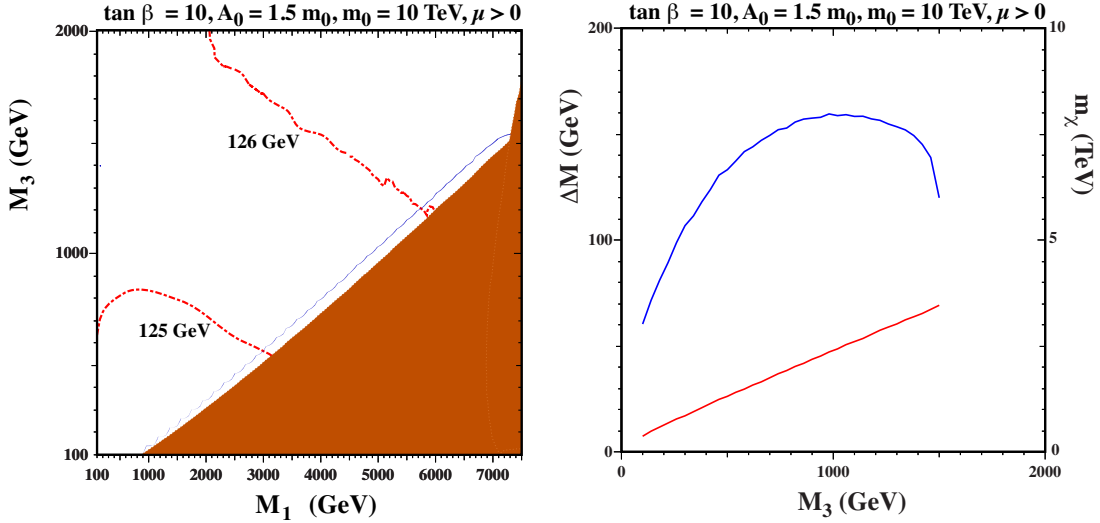
Figure 8: *As for Fig. 1, but for $m_0 = 10$ TeV, $\tan\beta = 10$ and $A_0/m_0 = 1.5$.*

These features also appear when $m_0 = 10$ TeV. In general, this scenario is constrained at small A_0/m_0 by the absence of electroweak symmetry breaking, and at large A_0/m_0 by m_H and the appearance of a stop LSP.

4 Pure Gravity Mediation with Vector Multiplets

Another possible way of realizing a spectrum that can lead to gluino coannihilation is in models with pure gravity mediation [38, 39, 40] of supersymmetry breaking with additional vector multiplets [22, 23]. The model we consider here is based on that in [23], whose setup we briefly review here. The effective potential is similar to that for the CMSSM:

$$V = \left| \frac{\partial W}{\partial \phi^i} \right|^2 + \left(A_0 W^{(3)} + B_0 W^{(2)} + h.c. \right) + m_{3/2}^2 \phi^i \phi_i^* , \tag{12}$$

where $W^{(3)}$ corresponds to the trilinear terms of the superpotential, $W^{(2)}$ contains the bilinear terms of the superpotential, and the ϕ_i signify the MSSM fields, with

$$W = \left(y_e H_1 L e^c + y_d H_1 Q d^c + y_u H_2 Q u^c \right) + \mu H_1 H_2 . \tag{13}$$

The scalar masses are generated through gravity mediation with a minimal Kähler potential, in an identical manner to mSUGRA [41], and hence are equal to $m_{3/2}$ at the GUT scale. In general, as seen in (12), the form of $W^{(3)}$ dictates the pattern of the trilinear supersymmetry-breaking terms. However, the trilinear couplings are suppressed in PGM models, because the supersymmetry-breaking field is charged. Thus, we take $A_0 = 0$.

13

Since $A_0 = 0$ and the Kähler potential is minimal in this model, we have $B_0 = -m_{3/2}$ for the Higgs fields. This leaves three free parameters, two of which are determined by enforcing the electroweak symmetry-breaking conditions;

$$\mu^2 = \frac{m_1^2 - m_2^2 \tan^2\beta + \frac{1}{2}m_Z^2(1 - \tan^2\beta) + \Delta_\mu^{(1)}}{\tan^2\beta - 1 + \Delta_\mu^{(2)}} \,, \tag{14}$$

and

$$B\mu = -\frac{1}{2}(m_1^2 + m_2^2 + 2\mu^2)\sin 2\beta + \Delta_B \,, \tag{15}$$

where $\Delta_\mu^{(1)}$, $\Delta_\mu^{(2)}$ and Δ_B are loop corrections to the relationships [42].

This scenario has a very restricted parameter space that does not, in general, realize electroweak symmetry breaking [40]. Therefore, we add a Giudice-Masiero (GM) term [43] for the Higgs fields, which modifies the GUT-scale values of both B_0 and μ:

$$\mu = \mu_0 + c_H m_{3/2} \,, \tag{16}$$
$$B\mu = -\mu_0 m_{3/2} + 2c_H m_{3/2}^2 \,. \tag{17}$$

This additional degree of freedom in the EWSB sector allows us to choose $\tan\beta$ (in addition to $m_{3/2}$) as a free parameter, and one finds viable parameter space as long as $\tan\beta \lesssim 3$ [40].

We consider here an extension of this simplest viable version of the PGM scenario that includes an additional $\mathbf{10}$ and $\overline{\mathbf{10}}$. Because these states are vector-like, the most general form of the Kähler potential will be

$$K = |\mathbf{10}|^2 + |\overline{\mathbf{10}}|^2 + \left(C_{10}(\mathbf{10} \cdot \overline{\mathbf{10}}) + h.c.\right) \,, \tag{18}$$

which includes a GM-like coupling C_{10} that generates a supersymmetric mixing mass term, μ_{10}, and a supersymmetry-breaking B term for the additional vector-like fields. Because of the minimal form of the kinetic terms in the limit $C_{10} \to 0$, the additional fields also have a gravity-mediated tree-level soft supersymmetry-breaking mass equal to $m_{3/2}$. Since the $\mathbf{10}$ contains fields with the same quantum numbers as SM fields, the $\mathbf{10}$ ($\overline{\mathbf{10}}$) can be combined into gauge-invariant operators with H_2 (H_1). If we impose only gauge symmetries the most generic contribution to the superpotential is

$$W = y_t' H_u Q'U' + y_b' H_d \bar{Q}\bar{U} \,, \tag{19}$$

where Q' and U' are from the $\mathbf{10}$ and $\bar{Q}$ and $\bar{U}$ are from the $\overline{\mathbf{10}}$. However, to preserve R symmetry we must take either $y_b' = 0$ or $y_t' = 0$. Here, we take $y_b' = 0$. The interactions

proportional to y'_t contribute to the beta function of the up Higgs soft mass in a similar way to those controlled by y_t. Specifying a comparable value of y'_t helps drive radiative electroweak symmetry breaking, which in turn allows larger values of $\tan\beta > 3$. The extended theory now has four parameters: $m_{3/2}$, $\tan\beta$, C_{10}, and y'_t.

The gaugino masses in the models are generated by anomalies [44]. Thus because the contributions to gaugino masses are proportional to $m_{3/2}$, scalar masses tend to be much heavier than the gaugino masses, reminiscent of split supersymmetry [45]. With the addition of the **10** and $\overline{\mathbf{10}}$ the anomaly-mediated contributions to the gaugino masses are

$$M_1 = \frac{48}{5}\frac{g_1^2}{16\pi^2}m_{3/2} \, , \tag{20}$$

$$M_2 = \frac{g_2^2}{4\pi^2}m_{3/2} \, , \tag{21}$$

$$M_3 = 0 \, . \tag{22}$$

In addition, the gauginos then get rather large threshold corrections from the **10** and $\overline{\mathbf{10}}$ when they are integrated out, which is in addition to the large threshold correction coming from integrating out the Higgsinos: for more details see [23]. Since the only contribution to the mass of the gluino comes from the threshold corrections, it tends to be lighter than in typical PGM models. Hence there are regions where the gluino can coannihilate with the bino, yielding the possibility of a relatively heavy dark matter candidate.

Our results for the PGM model with vector **10** and $\overline{\mathbf{10}}$ multiplets can be displayed in $(c_H, m_{3/2})$ planes for fixed values of the Yukawa coupling, y'_t and $\tan\beta$. Two examples of these planes are shown in Figs. 9 and 10. In the former, we have fixed $\tan\beta = 3$ (mainly to get an acceptable value for the Higgs mass, m_H, over the range of $m_{3/2} \le 600$ TeV shown) and $y'^2_t = 0.15$. In the left panel, we see a large red shaded region at small c_H where the gluino is the LSP. To the right of this boundary, we see the gluino coannihilation strip [2]. In the lower right corner, the pink shaded region is excluded because one or more of the new vector scalars becomes tachyonic. As in previous figures, the Higgs mass contours are shown as red dot-dashed curves as labelled. Within the theoretical uncertainties, the Higgs mass agrees with experiment over the part of the plane that is shown. In the right panel we see, as before, the gluino-neutralino mass difference ΔM along the gluino coannihilation strip (blue) and the neutralino mass along the strip (red). We see that the curve for ΔM has the same characteristic shape due to strong coannihilations involving the gluino and peaks at $\simeq 170$ GeV at $m_{3/2} \simeq 200$ TeV when $m_\chi \simeq 3$ TeV. The end-point of the coannihilation strip

---

[2]The strip becomes less well defined at $m_{3/2} \gtrsim 350$ TeV due to inaccuracies of the relic density calculation at such large masses.

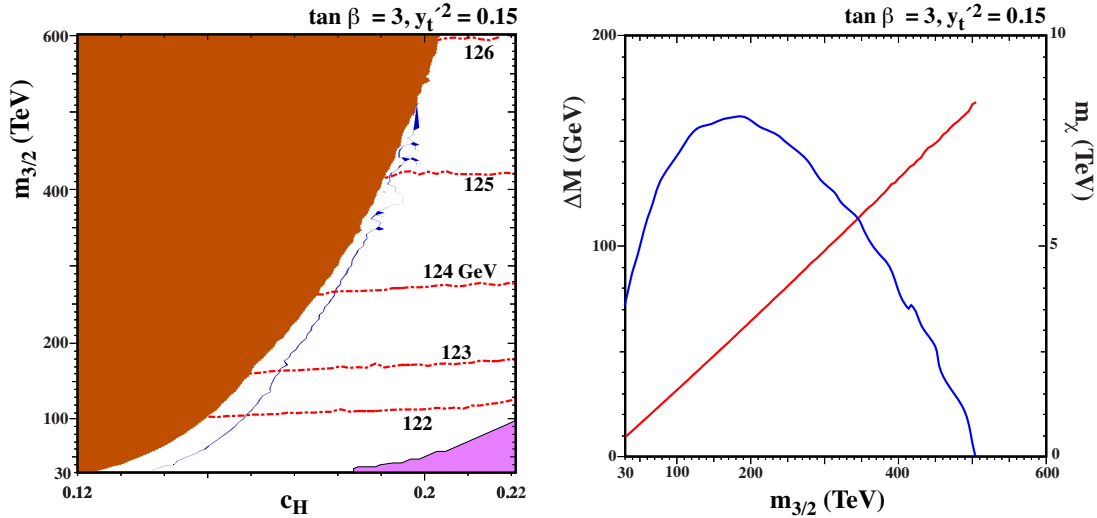occurs at $m_{3/2} \simeq 500$ TeV where $m_\chi \simeq 8.3$ TeV [3].

Figure 9: *The PGM $(c_H, m_{3/2})$ plane for fixed $\tan\beta = 3$ and $y_t'^2 = 0.15$. The dark blue strip in the left panel shows where the relic LSP density $\Omega_\chi h^2$ falls within the ± 3-σ range allowed by Planck and other data, and the lightest neutralino is no longer the LSP in the low-c_H regions shaded brick-red. One or more of the new vector scalars becomes tachyonic in the lower right corner of the plane (shaded pink). The right panel shows the gluino-neutralino mass difference (left axis, blue line) and the neutralino mass (right axis, red line) as functions of $m_{3/2}$.*

In Fig. 10, we show in the left panel corresponding $(c_H, m_{3/2})$ plane for fixed $y_t'^2 = 0.65$ and the same value of $\tan\beta = 3$. In this case with a higher Yukawa coupling, slightly higher c_H is needed to obtain a neutralino LSP. As in the previous case, we see a brick-red shaded gluino LSP for low c_H and, at slightly larger c_H, a gluino coannihilation strip. As previously, m_H is acceptable along all the displayed portion of the strip where $m_{3/2} \leq 400$ TeV. In this case, the region at larger c_H where one or more of the new vector scalars becomes tachyonic also extends to low c_H for small $m_{3/2}$. The right panel of Fig. 10 shows the values of ΔM and m_χ along the gluino coannihilation strip. In this case, we see that ΔM is maximized at ~ 160 GeV for $m_{3/2} \sim 150$ TeV. The end-point of the gluino coannihilation strip also occurs at $m_{3/2} \simeq 500$ TeV with m_χ around 8.3 TeV.

Finally, we show in Fig. 11 an example of a $(y_t'^2, c_H)$ plane with $\tan\beta = 5$ for four choices of the gravitino mass, namely $m_{3/2} = 30, 50, 100$ and 250 TeV. The red shaded region has a gluino LSP only in the $m_{3/2} = 30$ TeV case. In the other three cases this region would

---

[3]The maximal value of the LSP mass that is compatible with it being a viable dark matter candidate in this case is similar to the CMSSM case, even though there are additional squarks to mediate $\chi_0 q \rightarrow q\tilde{g}$. This is because the limiting reaction is gluino-gluino annihilation, which is the same in the two cases.
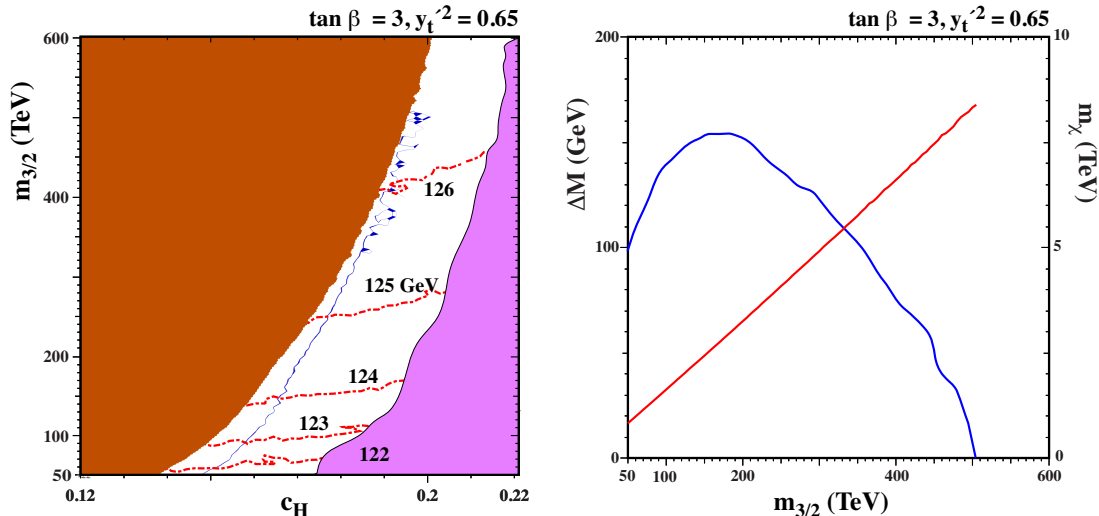
16

Figure 10: *As in Fig. 9, the PGM* $(c_H, m_{3/2})$ *plane for fixed* $\tan\beta = 3$ *and* $y_t'^2 = 0.65$.

be displaced to larger c_H. Because the Higgs mass depends on $m_{3/2}$, there are no unique contours that can be displayed for all four cases. Instead, we have color-coded the gluino coannihilation strip according to the Higgs mass: 124-125 GeV (black), 125-126 GeV (blue), 126-127 GeV (green), 127-128 GeV (red), and > 128 GeV (yellow) [4]. The right panel shows that the gluino-neutralino mass difference is almost independent of $y_t'^2$. We do not show the neutralino mass for these cases, as it is largely independent of y_t' and is determined from the gravitino mass and can be read from either of the two previous figures.

5   Summary and Conclusions

We have presented in this paper a couple of representative MSSM scenarios in which the gluino may be nearly degenerate with the neutralino LSP χ, whose relic dark matter density is brought into the range favoured by Planck and other data by gluino coannihilation. It had been shown previously that values of $m_\chi \lesssim 8$ TeV are in principle possible when gluino coannihilation is operative [26], and we have shown in this paper how such a possibility can be embedded within a scenario for non-universal soft supersymmetry breaking within the MSSM, on the one hand, and within a simple extension of the MSSM with pure gravitational mediation of soft supersymmetry breaking that includes a vector-like $\mathbf{10} + \overline{\mathbf{10}}$ multiplet pair, on the other hand.

In both scenarios, the upper bound on m_χ depends on the details of the models. In

---

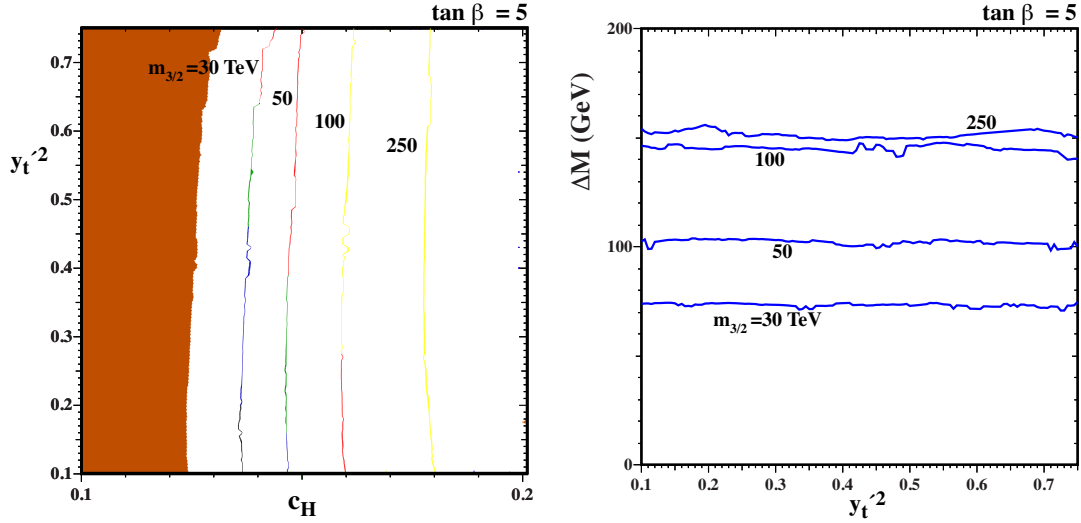[4] We recall also that the Higgs mass is sensitive to the choice of $\tan\beta$.

Figure 11: *The PGM $(y_t'^2, c_H)$ plane with $\tan\beta = 5$ for four choices of the gravitino mass, $m_{3/2} = 30, 50, 100$ and 250 TeV. The right panel shows the gluino-neutralino mass difference as a function of $y_t'^2$.*

particular, in the non-universal MSSM scenario there is competition from other mechanisms for bringing the dark matter density into the Planck range. These, together with other phenomenological constraints such as the mass of the Higgs boson and the requirement to ensure electroweak symmetry breaking, restrict the parameter region where gluino coannihilation is dominant. In the PGM scenario with extra vector-like multiplets, the allowed range of m_χ depends on the gravitino mass as well as a vector-like Yukawa coupling. In both cases, values of $m_\chi \sim 8$ TeV are quite possible.

Gluino coannihilation therefore offers the possibility that the LSP, and hence the rest of the supersymmetric spectrum, may lie in the multi-TeV range, beyond the reach of the LHC. Of course, we sincerely hope, if not expect, that supersymmetry will be discovered during future LHC runs. That said, the scenarios discussed here illustrate one way in which detection at the LHC could be evaded. An interesting and important question that lies beyond the scope of this paper is how to detect supersymmetry in a gluino coannihilation scenario with a multi-TeV LSP (see, e.g., the discussion in [46]). As we have discussed in this paper, the gluino-neutralino mass difference in such a scenario is typically $\mathcal{O}(100)$ GeV, resulting in a suppressed missing-energy signature whose detection at a future 100-TeV proton-proton collider might be challenging.

Une affaire à suivre.

Acknowledgements

References

[1] G. Aad *et al.* [ATLAS Collaboration], JHEP **1409** (2014) 176 [arXiv:1405.7875 [hep-ex]]; arXiv:1507.05525 [hep-ex]; full ATLAS Run 1 results can be found at `https://twiki.cern.ch/twiki/bin/view/AtlasPublic/SupersymmetryPublicResults`.

[2] S. Chatrchyan *et al.* [CMS Collaboration], JHEP **1406** (2014) 055 [arXiv:1402.4770 [hep-ex]]; full CMS Run 1 results can be found at `https://twiki.cern.ch/twiki/bin/view/CMSPublic/PhysicsResultsSUS`.

[3] The ATLAS collaboration, ATLAS-CONF-2015-026; CMS Collaboration [CMS Collaboration], CMS-PAS-SUS-14-003.

[4] CMS Collaboration [CMS Collaboration], CMS-PAS-SUS-14-019.

[5] S. P. Martin, Phys. Rev. D **75**, 115005 (2007) [hep-ph/0703097 [HEP-PH]]; B. Bhattacherjee, A. Choudhury, K. Ghosh and S. Poddar, Phys. Rev. D **89**, no. 3, 037702 (2014) [arXiv:1308.1526 [hep-ph]].

[6] O. Buchmueller, M. Citron, J. Ellis, S. Guha, J. Marrouche, K. A. Olive, K. de Vries and J. Zheng, Eur. Phys. J. C **75** (2015) 10, 469 [arXiv:1505.04702 [hep-ph]].

[7] H. Goldberg, Phys. Rev. Lett. **50** (1983) 1419; J. Ellis, J. Hagelin, D. Nanopoulos, K. Olive and M. Srednicki, Nucl. Phys. B **238** (1984) 453.

[8] P. A. R. Ade *et al.* [Planck Collaboration], arXiv:1502.01589 [astro-ph.CO].

[9] J. Ellis and K. A. Olive, Eur. Phys. J. C **72**, 2005 (2012) [arXiv:1202.3262 [hep-ph]].

[10] J. Ellis, F. Luo, K. A. Olive and P. Sandick, Eur. Phys. J. C **73**, no. 4, 2403 (2013) [arXiv:1212.4476 [hep-ph]]; J. Ellis, J. L. Evans, F. Luo, N. Nagata, K. A. Olive and P. Sandick, arXiv:1509.08838 [hep-ph].

[11] E. A. Bagnaschi *et al.*, arXiv:1508.01173 [hep-ph].

[12] L. Aparicio, D. G. Cerdeno and L. E. Ibanez, JHEP **1204**, 126 (2012) [arXiv:1202.0822 [hep-ph]]; H. Baer, V. Barger and A. Mustafayev, JHEP **1205** (2012) 091 [arXiv:1202.4038 [hep-ph]]; P. Bechtle, T. Bringmann, K. Desch, H. Dreiner, M. Hamer, C. Hensel, M. Kramer and N. Nguyen *et al.*, JHEP **1206**, 098 (2012) [arXiv:1204.4199 [hep-ph]]; C. Balazs, A. Buckley, D. Carter, B. Farmer and M. White, arXiv:1205.1568 [hep-ph]; D. Ghosh, M. Guchait, S. Raychaudhuri and D. Sengupta, Phys. Rev. D **86**, 055007 (2012) [arXiv:1205.2283 [hep-ph]]; A. Fowlie, M. Kazana, K. Kowalska, S. Munir, L. Roszkowski, E. M. Sessolo, S. Trojanowski and Y. -L. S. Tsai, Phys. Rev. D **86**, 075010 (2012) [arXiv:1206.0264 [hep-ph]]; K. Kowalska *et al.* [BayesFITS Group Collaboration], Phys. Rev. D **87**, no. 11, 115010 (2013) [arXiv:1211.1693 [hep-ph]]; C. Strege, G. Bertone, F. Feroz, M. Fornasa, R. Ruiz de Austri and R. Trotta, JCAP **1304**, 013 (2013) [arXiv:1212.2636 [hep-ph]]; M. E. Cabrera, J. A. Casas and R. R. de Austri, JHEP **1307** (2013) 182 [arXiv:1212.4821 [hep-ph]]; T. Cohen and J. G. Wacker, JHEP **1309** (2013) 061 [arXiv:1305.2914 [hep-ph]]; S. Henrot-Versill, Rm. Lafaye, T. Plehn, M. Rauch, D. Zerwas, S. p. Plaszczynski, B. Rouill d'Orfeuil and M. Spinelli, Phys. Rev. D **89**, 055017 (2014) [arXiv:1309.6958 [hep-ph]]; P. Bechtle, K. Desch, H. K. Dreiner, M. Hamer, M. Krer, B. O'Leary, W. Porod and X. Prudent *et al.*, arXiv:1310.3045 [hep-ph]; L. Roszkowski, E. M. Sessolo and A. J. Williams, JHEP **1408**, 067 (2014) [arXiv:1405.4289 [hep-ph]]; P. Bechtle *et al.*, arXiv:1508.05951 [hep-ph].

[13] M. Drees and M. M. Nojiri, Phys. Rev. D **47** (1993) 376 [arXiv:hep-ph/9207234]; H. Baer and M. Brhlik, Phys. Rev. D **53** (1996) 597 [arXiv:hep-ph/9508321]; Phys. Rev. D **57** (1998) 567 [arXiv:hep-ph/9706509]; H. Baer, M. Brhlik, M. A. Diaz, J. Ferrandis, P. Mercadante, P. Quintana and X. Tata, Phys. Rev. D **63** (2001) 015007 [arXiv:hep-ph/0005027]; J. R. Ellis, T. Falk, G. Ganis, K. A. Olive and M. Srednicki, Phys. Lett. B **510** (2001) 236 [arXiv:hep-ph/0102098].

[14] K. Griest and D. Seckel, Phys. Rev. D **43**, 3191 (1991).

[15] J. Ellis, T. Falk, and K.A. Olive, Phys. Lett. **B444** (1998) 367 [arXiv:hep-ph/9810360]; J. Ellis, T. Falk, K.A. Olive, and M. Srednicki, *Astr. Part. Phys.* **13** (2000) 181

[Erratum-ibid. **15** (2001) 413] [arXiv:hep-ph/9905481]; R. Arnowitt, B. Dutta and Y. Santoso, Nucl. Phys. B **606** (2001) 59 [arXiv:hep-ph/0102181]; M. E. Gómez, G. Lazarides and C. Pallis, Phys. Rev. D **D61** (2000) 123512 [arXiv:hep-ph/9907261]; Phys. Lett. **B487** (2000) 313 [arXiv:hep-ph/0004028]; Nucl. Phys. B **B638** (2002) 165 [arXiv:hep-ph/0203131]; T. Nihei, L. Roszkowski and R. Ruiz de Austri, JHEP **0207** (2002) 024 [arXiv:hep-ph/0206266]; M. Citron, J. Ellis, F. Luo, J. Marrouche, K. A. Olive and K. J. de Vries, Phys. Rev. D **87**, 036012 (2013) [arXiv:1212.2886 [hep-ph]].

[16] C. Boehm, A. Djouadi and M. Drees, Phys. Rev. D **62**, 035012 (2000) [arXiv:hep-ph/9911496]; J. R. Ellis, K. A. Olive and Y. Santoso, Astropart. Phys. **18**, 395 (2003) [arXiv:hep-ph/0112113]; J. L. Diaz-Cruz, J. R. Ellis, K. A. Olive and Y. Santoso, JHEP **0705**, 003 (2007) [arXiv:hep-ph/0701229]; I. Gogoladze, S. Raza and Q. Shafi, Phys. Lett. B **706**, 345 (2012) [arXiv:1104.3566 [hep-ph]]; M. A. Ajaib, T. Li and Q. Shafi, Phys. Rev. D **85**, 055021 (2012) [arXiv:1111.4467 [hep-ph]]; J. Harz, B. Herrmann, M. Klasen, K. Kovarik and Q. L. Boulc'h, Phys. Rev. D **87** (2013) 5, 054031 [arXiv:1212.5241]; J. Harz, B. Herrmann, M. Klasen and K. Kovarik, Phys. Rev. D **91** (2015) 3, 034028 [arXiv:1409.2898 [hep-ph]]; J. Ellis, K. A. Olive and J. Zheng, Eur. Phys. J. C **74**, 2947 (2014) [arXiv:1404.5571 [hep-ph]]; A. Ibarra, A. Pierce, N. R. Shah and S. Vogl, Phys. Rev. D **91**, no. 9, 095018 (2015) [arXiv:1501.03164 [hep-ph]].

[17] J. Edsjo, M. Schelke, P. Ullio and P. Gondolo, JCAP **0304**, 001 (2003) [hep-ph/0301106].

[18] S. Raza, Q. Shafi and C. S. n, Phys. Rev. D **92**, no. 5, 055010 (2015) [arXiv:1412.7672 [hep-ph]].

[19] S. Mizuta and M. Yamaguchi, Phys. Lett. B **298** (1993) 120 [arXiv:hep-ph/9208251]; J. Edsjo and P. Gondolo, Phys. Rev. D **56**, 1879 (1997) [hep-ph/9704361]; H. Baer, C. Balazs and A. Belyaev, JHEP **0203**, 042 (2002) [hep-ph/0202076]; A. Birkedal-Hansen and E. h. Jeong, JHEP **0302**, 047 (2003) [hep-ph/0210041].

[20] S. Profumo and C. E. Yaguna, Phys. Rev. D **69**, 115009 (2004) [hep-ph/0402208]; D. Feldman, Z. Liu and P. Nath, Phys. Rev. D **80**, 015007 (2009) [arXiv:0905.1148 [hep-ph]]; N. Chen, D. Feldman, Z. Liu, P. Nath and G. Peim, Phys. Rev. D **83**, 035005 (2011) [arXiv:1011.1246 [hep-ph]].

[21] I. Gogoladze, R. Khalid and Q. Shafi, Phys. Rev. D **79**, 115004 (2009) [arXiv:0903.5204 [hep-ph]]; I. Gogoladze, R. Khalid and Q. Shafi, Phys. Rev. D **80**, 095016 (2009)

[arXiv:0908.0731 [hep-ph]]; M. Adeel Ajaib, T. Li, Q. Shafi and K. Wang, JHEP **1101**, 028 (2011) [arXiv:1011.5518 [hep-ph]].

[22] K. Harigaya, M. Ibe and T. T. Yanagida, JHEP **1312**, 016 (2013) [arXiv:1310.0643 [hep-ph]]; K. Harigaya, K. Kaneta and S. Matsumoto, Phys. Rev. D **89**, no. 11, 115021 (2014) [arXiv:1403.0715 [hep-ph]].

[23] J. L. Evans and K. A. Olive, Phys. Rev. D **90**, no. 11, 115020 (2014) [arXiv:1408.5102 [hep-ph]].

[24] A. De Simone, G. F. Giudice and A. Strumia, JHEP **1406**, 081 (2014) [arXiv:1402.6287 [hep-ph]].

[25] M. Low and L. T. Wang, JHEP **1408**, 161 (2014) [arXiv:1404.0682 [hep-ph]].

[26] J. Ellis, F. Luo and K. A. Olive, JHEP **1509**, 127 (2015) [arXiv:1503.07142 [hep-ph]].

[27] G. L. Kane, C. F. Kolda, L. Roszkowski and J. D. Wells, Phys. Rev. D **49** (1994) 6173 [arXiv:hep-ph/9312272]; J. R. Ellis, T. Falk, K. A. Olive and M. Schmitt, Phys. Lett. B **388** (1996) 97 [arXiv:hep-ph/9607292]; Phys. Lett. B **413** (1997) 355 [arXiv:hep-ph/9705444]; V. D. Barger and C. Kao, Phys. Rev. D **57** (1998) 3131 [arXiv:hep-ph/9704403]; L. Roszkowski, R. Ruiz de Austri and T. Nihei, JHEP **0108** (2001) 024 [arXiv:hep-ph/0106334]; A. Djouadi, M. Drees and J. L. Kneur, JHEP **0108** (2001) 055 [arXiv:hep-ph/0107316]; U. Chattopadhyay, A. Corsetti and P. Nath, Phys. Rev. D **66** (2002) 035003 [arXiv:hep-ph/0201001]; J. R. Ellis, K. A. Olive and Y. Santoso, New Jour. Phys. **4** (2002) 32 [arXiv:hep-ph/0202110]; H. Baer, C. Balazs, A. Belyaev, J. K. Mizukoshi, X. Tata and Y. Wang, JHEP **0207** (2002) 050 [arXiv:hep-ph/0205325]; R. Arnowitt and B. Dutta, arXiv:hep-ph/0211417.

[28] J. R. Ellis, T. Falk, G. Ganis, K. A. Olive and M. Schmitt, Phys. Rev. D **58** (1998) 095002 [arXiv:hep-ph/9801445]; J. R. Ellis, T. Falk, G. Ganis and K. A. Olive, Phys. Rev. D **62** (2000) 075010 [arXiv:hep-ph/0004169].

[29] J. R. Ellis, K. A. Olive, Y. Santoso and V. C. Spanos, Phys. Lett. B **565** (2003) 176 [arXiv:hep-ph/0303043]; H. Baer and C. Balazs, JCAP **0305**, 006 (2003) [arXiv:hep-ph/0303114]; A. B. Lahanas and D. V. Nanopoulos, Phys. Lett. B **568**, 55 (2003) [arXiv:hep-ph/0303130]; U. Chattopadhyay, A. Corsetti and P. Nath, Phys. Rev. D **68**, 035005 (2003) [arXiv:hep-ph/0303201]; C. Munoz, Int. J. Mod. Phys. A **19**, 3093 (2004) [arXiv:hep-ph/0309346]; R. Arnowitt, B. Dutta and B. Hu,

arXiv:hep-ph/0310103; J. Ellis and K. A. Olive, arXiv:1001.3651 [astro-ph.CO], published in *Particle dark matter*, ed. G. Bertone, pp. 142-163.

[30] O. Buchmueller *et al.*, Eur. Phys. J. C **74** (2014) 3, 2809 [arXiv:1312.5233 [hep-ph]].

[31] D. Matalliotakis and H. P. Nilles, Nucl. Phys. B **435** (1995) 115 [arXiv:hep-ph/9407251]; M. Olechowski and S. Pokorski, Phys. Lett. B **344**, 201 (1995) [arXiv:hep-ph/9407404]; V. Berezinsky, A. Bottino, J. Ellis, N. Fornengo, G. Mignola and S. Scopel, *Astropart. Phys.* **5** (1996) 1, hep-ph/9508249; M. Drees, M. Nojiri, D. Roy and Y. Yamada, *Phys. Rev.* **D 56** (1997) 276, [Erratum-ibid. **D 64** (1997) 039901], hep-ph/9701219; M. Drees, Y. Kim, M. Nojiri, D. Toya, K. Hasuko and T. Kobayashi, *Phys. Rev.* **D 63** (2001) 035008, hep-ph/0007202; P. Nath and R. Arnowitt, *Phys. Rev.* **D 56** (1997) 2820, hep-ph/9701301; A. Bottino, F. Donato, N. Fornengo and S. Scopel, *Phys. Rev.* **D 63** (2001) 125003, hep-ph/0010203; S. Profumo, *Phys. Rev.* **D 68** (2003) 015006, hep-ph/0304071; D. Cerdeno and C. Munoz, *JHEP* **0410** (2004) 015, hep-ph/0405057.

[32] J. Ellis, K. Olive and Y. Santoso, Phys. Lett. B **539**, 107 (2002) [arXiv:hep-ph/0204192]; J. R. Ellis, T. Falk, K. A. Olive and Y. Santoso, Nucl. Phys. B **652**, 259 (2003) [arXiv:hep-ph/0210205].

[33] H. Baer, A. Mustafayev, S. Profumo, A. Belyaev and X. Tata, Phys. Rev. D **71**, 095008 (2005) [arXiv:hep-ph/0412059]; H. Baer, A. Mustafayev, S. Profumo, A. Belyaev and X. Tata, *JHEP* **0507** (2005) 065, hep-ph/0504001.

[34] J. R. Ellis, K. A. Olive and P. Sandick, Phys. Rev. D **78**, 075012 (2008) [arXiv:0805.2343 [hep-ph]].

[35] G. F. Giudice and A. Strumia, Nucl. Phys. B **858**, 63 (2012) [arXiv:1108.6077 [hep-ph]]; E. Bagnaschi, G. F. Giudice, P. Slavich and A. Strumia, JHEP **1409**, 092 (2014) [arXiv:1407.4081 [hep-ph]].

[36] J. L. Feng, K. T. Matchev and T. Moroi, Phys. Rev. Lett. **84**, 2322 (2000) [arXiv:hep-ph/9908309]; Phys. Rev. D **61**, 075005 (2000) [arXiv:hep-ph/9909334]; J. L. Feng, K. T. Matchev and F. Wilczek, Phys. Lett. B **482**, 388 (2000) [arXiv:hep-ph/0004043]; H. Baer, T. Krupovnickas, S. Profumo and P. Ullio, JHEP **0510** (2005) 020 [hep-ph/0507282]; J. L. Feng, K. T. Matchev and D. Sanford, Phys. Rev. D **85**, 075007 (2012) [arXiv:1112.3021 [hep-ph]]; P. Draper, J. Feng, P. Kant, S. Profumo and D. Sanford, Phys. Rev. D **88**, 015025 (2013) [arXiv:1304.1159 [hep-ph]].

[37] N. Arkani-Hamed, A. Delgado and G. F. Giudice, Nucl. Phys. B **741** (2006) 108 [hep-ph/0601041].

[38] M. Ibe, T. Moroi and T. T. Yanagida, Phys. Lett. B **644**, 355 (2007) [hep-ph/0610277]; M. Ibe and T. T. Yanagida, Phys. Lett. B **709**, 374 (2012) [arXiv:1112.2462 [hep-ph]]; M. Ibe, S. Matsumoto and T. T. Yanagida, Phys. Rev. D **85**, 095011 (2012) [arXiv:1202.2253 [hep-ph]].

[39] L. J. Hall and Y. Nomura, JHEP **1201**, 082 (2012) [arXiv:1111.4519 [hep-ph]]; N. Arkani-Hamed, A. Gupta, D. E. Kaplan, N. Weiner and T. Zorawski, arXiv:1212.6971 [hep-ph]; A. Arvanitaki, N. Craig, S. Dimopoulos and G. Villadoro, JHEP **1302**, 126 (2013) [arXiv:1210.0555 [hep-ph]]; L. J. Hall, Y. Nomura and S. Shirai, JHEP **1301**, 036 (2013) [arXiv:1210.2395 [hep-ph]].

[40] J. L. Evans, M. Ibe, K. A. Olive and T. T. Yanagida, Eur. Phys. J. C **73**, 2468 (2013) [arXiv:1302.5346 [hep-ph]].

[41] R. Barbieri, S. Ferrara and C. A. Savoy, Phys. Lett. B **119**, 343 (1982).

[42] V. D. Barger, M. S. Berger and P. Ohmann, Phys. Rev. D **49** (1994) 4908 [arXiv:hep-ph/9311269]; W. de Boer, R. Ehret and D. I. Kazakov, Z. Phys. C **67** (1995) 647 [arXiv:hep-ph/9405342]; M. Carena, J. R. Ellis, A. Pilaftsis and C. E. Wagner, Nucl. Phys. B **625** (2002) 345 [arXiv:hep-ph/0111245].

[43] G. F. Giudice and A. Masiero, Phys. Lett. B **206**, 480 (1988); K. Inoue, M. Kawasaki, M. Yamaguchi and T. Yanagida, Phys. Rev. D **45**, 328 (1992); E. Dudas, Y. Mambrini, A. Mustafayev and K. A. Olive, Eur. Phys. J. C **72**, 2138 (2012) [arXiv:1205.5988 [hep-ph]].

[44] M. Dine and D. MacIntire, Phys. Rev. D **46**, 2594 (1992) [hep-ph/9205227]; L. Randall and R. Sundrum, Nucl. Phys. B **557**, 79 (1999) [arXiv:hep-th/9810155]; G. F. Giudice, M. A. Luty, H. Murayama and R. Rattazzi, JHEP **9812**, 027 (1998) [arXiv:hep-ph/9810442]; J. A. Bagger, T. Moroi and E. Poppitz, JHEP **0004**, 009 (2000) [arXiv:hep-th/9911029]; P. Binetruy, M. K. Gaillard and B. D. Nelson, Nucl. Phys. B **604**, 32 (2001) [arXiv:hep-ph/0011081].

[45] J. D. Wells, hep-ph/0306127; N. Arkani-Hamed and S. Dimopoulos, JHEP **0506**, 073 (2005) [arXiv:hep-th/0405159]; G. F. Giudice and A. Romanino, Nucl. Phys. B

699, 65 (2004) [Erratum-ibid. B **706**, 65 (2005)] [arXiv:hep-ph/0406088]; N. Arkani-Hamed, S. Dimopoulos, G. F. Giudice and A. Romanino, Nucl. Phys. B **709**, 3 (2005) [arXiv:hep-ph/0409232]; J. D. Wells, Phys. Rev. D **71**, 015013 (2005) [arXiv:hep-ph/0411041].

[46] N. Nagata, H. Otono and S. Shirai, Phys. Lett. B **748** (2015) 24 [arXiv:1504.00504 [hep-ph]].